

Article

A New 1 Bit Electronically Reconfigurable Transmitarray

Zizhen Zheng, Wu Ren , Weiming Li and Zhenghui Xue

School of Integrated Circuits and Electronics, Beijing Institute of Technology, Beijing 100081, China; bitzhengzizhen@163.com (Z.Z.); wml@bit.edu.cn (W.L.); zhxue@bit.edu.cn (Z.X.)

* Correspondence: renwu@bit.edu.cn

Abstract: This article proposes a novel 1 bit electronically reconfigurable transmitarray, designed to facilitate digital two-dimensional beam scanning, boasting both high gain and a slim profile. The fundamental phase shifting unit of the transmitarray unit cell consists of a resonant cavity composed of a pair of orthogonal metal gates and dielectric layers, with a cross-sectional height of 0.17λ . The middle layer of the phase-shifting unit is composed of circular gaps and C-shaped patches, and two diodes with opposite directions are loaded. By turning the diodes ON and OFF, current reversal is accomplished, allowing the unit to transition between its 0 and 1 states and achieve transmission-phase quantization. The unit's minimal insertion loss is 0.37 dB in state 0 and 0.35 dB in state 1, respectively. In order to verify our design, we designed and processed a 16×16 transmitarray in the C-band. The simulated results are consistent with the experimental results. The experimental results show that the transmitarray can achieve $\pm 45^\circ$ beam scanning on both the E-plane and H-plane, and the maximum gain is 20.59 dBi at 5 GHz, with an aperture efficiency of 20.5%.

Keywords: transmitarray; reconfigurable; beam scanning



Citation: Zheng, Z.; Ren, W.; Li, W.; Xue, Z. A New 1 Bit Electronically Reconfigurable Transmitarray. *Electronics* **2024**, *13*, 1383. <https://doi.org/10.3390/electronics13071383>

Academic Editor: Christos J. Bouras

Received: 11 March 2024

Revised: 1 April 2024

Accepted: 3 April 2024

Published: 5 April 2024



Copyright: © 2024 by the authors. Licensee MDPI, Basel, Switzerland. This article is an open access article distributed under the terms and conditions of the Creative Commons Attribution (CC BY) license (<https://creativecommons.org/licenses/by/4.0/>).

1. Introduction

Beam-scanning technology plays a pivotal role in enhancing the target tracking capabilities of radar, communication, and navigation systems. Traditionally, this functionality has been achieved through phased array antennas, which manipulate the beam direction by adjusting the phase difference between individual antenna units. However, the design of transmit/receive (T/R) modules for phased array antennas is complex, expensive, and requires the design of complex phase-shifting network [1,2]. Recent advancements in antenna technology have seen the emergence of reconfigurable metasurfaces as a promising alternative. Distinguished by their ability to dynamically alter operating modes and achieve multiple radiation patterns on the same platform, reconfigurable metasurfaces offer several advantages over traditional approaches. These include reduced antenna sizes, lower costs, and enhanced system integration capabilities [3]. Therefore, reconfigurable metasurfaces which include reflectarrays and transmitarrays have become a research hotspot in the field of antenna theory and technology. The pursuit of reconfigurability has led to innovations in mechanical structures as well as the adoption of tunable devices such as MEMS switches [4], varactor diodes [5], and particularly PIN diodes, due to their low cost, mature technology, and straightforward design [6,7]. PIN diodes have been extensively utilized to enhance the reconfigurability of antennas, contributing to advancements in beam-switching and scanning capabilities, and the development of dual-polarization [8] and 2 bit circularly polarized [9] beams. Despite these innovations, the reflectarray approach has been limited by its narrow bandwidth [10,11] and feed shielding issues, which compromise performance. The transmitarray, devoid of feed shielding problems, represents a significant step forward.

There are some reconfigurable transmitarray (RTA) designs that have shown good performances such as linear polarization, dual-linear polarization, and wide-angle beam scanning. A linear polarization RTA has been proposed by Antonio Clemente et al. They utilized the structure of U-shaped and O-shaped grooves, connected with metal via holes,

and achieved 1 bit phase control by loading a PIN diode [12]. Nguyen's team proposed a C-shaped patch and a C-shaped coupling groove [3,13], and loaded PIN diodes into the gap to achieve a 1 bit linear polarization transmission metasurface design in the X-band. In 2021, they accomplished 1 bit transmission in the Ka-band by putting metal through holes [14]. Min Wang et al. proposed integrating PIN diodes in the C-shaped microstrip feed layer, thereby achieving a good radiation performance [15]. In order to achieve a stable wide-angle beam scanning performance, reference [16] proposed an equivalent magnetic dipole unit structure, with a gain loss of only 3.6 dB for the 60° scanned beam in the E-plane. In order to achieve dual-linear polarization, Ref. [17] proposes a receiver–transmitter structure with an active receiving dipole and a passive asymmetric transmitting dipole. Ref. [18] uses space wave coupled to the feeder through gaps, and then achieves a 180° phase shift by selecting different paths. Finally, a linearly polarized wave is emitted through the gap, which is orthogonal to the direction of the incoming polarization wave. In reference [19], the author uses slot waveguide feeding instead of air feeding to achieve a reduction in the overall height profile. In these cases, active devices are typically used to reverse the current in order to produce the unit's phase difference. However, there is a problem with the above design structure. The receiving layer receives electromagnetic energy and transforms it into guided waves. These waves are then phase-shifted via tunable devices and radiated out through the radiating layer. As a result, tunable devices will receive practically all of the electromagnetic power, leading to large Ohmic losses. Research on how to realize low Ohmic loss structures to raise the array's aperture efficiency has long been a challenge for transmitarrays.

Polarization conversion has also been studied and applied in some research. Nathaniel's team proposed a polarization conversion reflective and transmissive metasurface in the terahertz band, which utilizes an oblique metal cut wire array to achieve a reflective polarization converter. It can convert linearly polarized electromagnetic waves into orthogonal linearly polarized electromagnetic waves, and has the characteristics of a wide frequency band and a high polarization conversion rate [20]. Ref. [21] introduces a polarization conversion with excellent roll-off features, an ultra-thin thickness, low insertion losses, and wide rejection bands. By designing a transmission structure based on polarization conversion and amplitude, a phase-independent adjustable transmitarray is realized [22], which has the characteristics of a low profile and low cost. A novel transmitarray structure is proposed in [23] that achieves line polarization to cross polarization through orthogonal polarization gates and a middle rectangular gap, and can achieve 2D beam scanning. In the above structural designs, the flat-phase shift characteristic required is achieved using polarization conversion.

This article introduces a 1 bit electronically reconfigurable transmitarray designed for 2D beam scanning in the C-band with a high efficiency and low loss. Through the use of a polarization conversion made up of dielectric layers and orthogonal metal gates, along with two reverse PIN diodes inserted in the middle, our design is able to produce a 180° phase difference. The "Unit Cell" section has a thorough structural description. A 16 × 16 transmitarray prototype validates the concept, demonstrating the ability to perform ±45° two-dimensional beam scanning on both the E-plane and H-plane with a maximum gain of 20.59 dBi. This research contributes to the field by addressing the limitations of previous designs and offering a streamlined, cost-effective solution for dynamic beam scanning.

2. Design and Optimization of Proposed Unit Cell

For reconfigurable transmitarrays, phase control must be achieved while maintaining a high level of transmittance. Therefore, in transmission design, not only should phase characteristics be considered, but transmission amplitude should also be taken into account. The foundational aspect of developing a 1 bit electronically reconfigurable transmitarray is the creation of a unit cell that is capable of incorporating active devices to facilitate a 180-degree phase shift. Our approach employs PIN diodes for dynamic phase shift control within the transmitarray unit, capitalizing on their cost-effectiveness and simplistic design. Typically, transmitarray elements are constructed from multi-layer frequency selective surfaces (FSS) or receive–transmit (Rx-Tx) structures. Achieving a comprehensive 360° phase shift with FSS

demands multiple layers [24], complicating integration and enlarging the transmitarray's overall volume. The receive–reradiate (Rx-Tx) structure is the most commonly used structure in the design of reconfigurable transmitarray. Its unit structure usually includes a receiving layer and a radiating layer, which are then connected through metals via holes or coupling gaps. However, traditional Rx-Tx architectures suffer from a limited bandwidth and notable losses. The structure proposed in this article circumvents these limitations.

2.1. Unit Cell

As shown in Figure 1a, the side length P of the unit-cell is 25 mm, slightly less than $0.5 \lambda_0$ at 5 GHz, where λ_0 is the free space wavelength. The unit cell consists of two layers of F4B ($\epsilon_r = 2.65, \tan \delta = 0.001$) substrate composition. The height of the top layer substrate is $h_1 = 1.5$ mm, and the height of the bottom layer substrate is $h_2 = 3$ mm. The interval between the top and bottom substrates is air with a height of $h_{air} = 5$ mm. There is an orthogonal metal polarization grating on the top and bottom layers of the medium, with a width of $W_2 = 3.6$ mm and a gap of $g = 1.6$ mm. In order to achieve the phase shift, a C-shaped structure is designed to be in the middle layer as shown in Figure 1b. As shown, in order to achieve the phase shift, a circular gap has been designed and two rectangular gaps are designed to be on the circular patch. The angles between these two rectangular gaps and the y -axis are $\pm 45^\circ$. Two diodes with opposite directions are installed on the gap, and their model is SMP1340-040LF of Skyworks Solutions Inc. When setting the feeding voltage, there is always only one diode in the ON state. When the diode is connected, the equivalent circuit is a series resistor and inductor, with $R = 1 \Omega$ and $L = 0.45$ nH; when the diode is OFF in reverse, the equivalent circuit is a series of a resistor, inductor, and capacitor, with $R = 10 \Omega$, $L = 0.45$ nH, and $C = 126$ fF.

The results obtained using the HFSS master–slave boundary condition and Floquet ports to simulate the unit cell are shown in Figure 2. It can be seen that, in the range of 4.7–5.3 GHz, the transmission loss is low ($S_{21} > -3$ dB). We refer to the situation where Diode 1 is OFF and Diode 2 is On as State 0, and the situation where Diode 1 is On and Diode 2 is OFF as State 1. From the simulation results, it can be seen that there is almost no difference in the S_{21} amplitudes between state 0 and state 1, with only a phase difference of 180° . Moreover, the phase response curve has a good linearity, and the phase difference remains constant within the operating frequency band. An air layer is positioned between the top and bottom layers in order to position the diodes. To achieve an optimal transmission performance, the air layer's height h_{air} is swept. As shown in Figure 3, it can be seen that, with the increase in h_{air} , the transmission loss of the unit cell gradually decreases. In the end, we settled on $h_{air} = 5$ mm since it has a decent transmission coefficient within the useful frequency range.

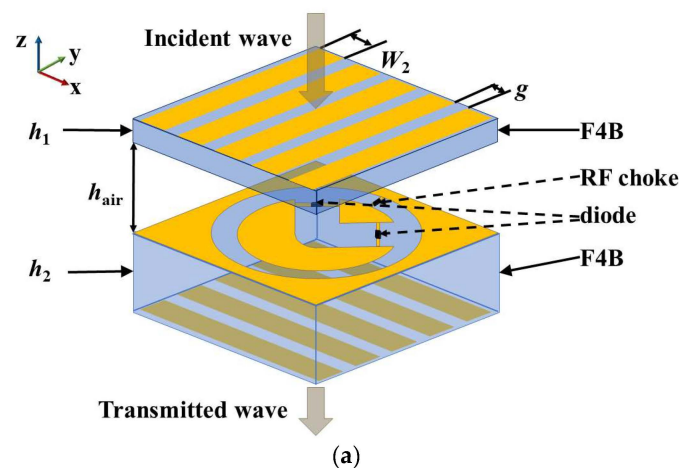


Figure 1. Cont.

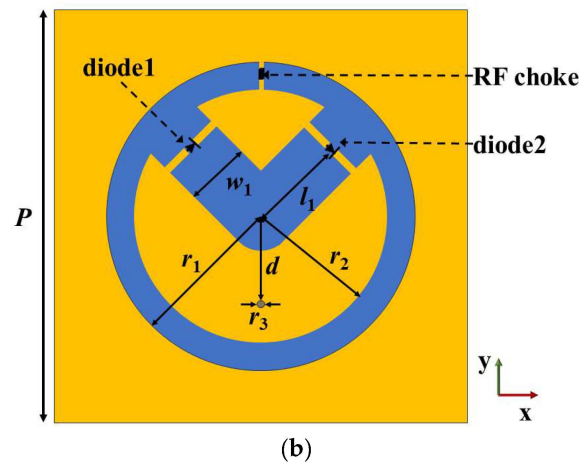


Figure 1. The structure of unit cell: (a) overall structure of the unit. (b) top view of the middle layer of the unit-cell.

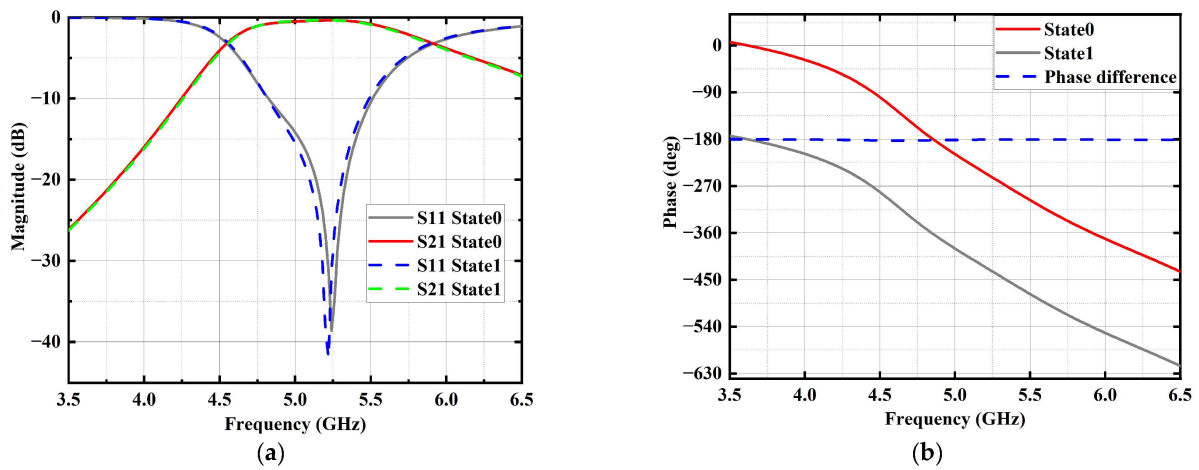


Figure 2. The transmission amplitude and phase of the unit cell: (a) transmission coefficient (S_{21}) and reflection coefficient (S_{11}). (b) Phase shift.

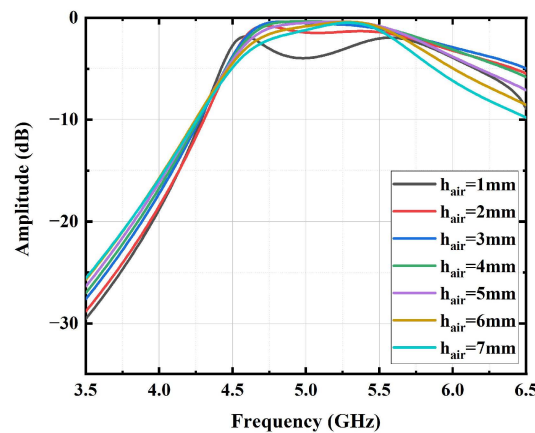


Figure 3. The transmission coefficient of the unit cell corresponding to different h_{air} .

A Fabry–Pérot cavity is an optical resonant cavity composed of two parallel highly reflective mirrors (or reflective surfaces), through which electromagnetic waves bounce back and forth, generating interference. The unit cell designed in this article consists of two orthogonal layers of metal gratings and a metal layer with a diagonal symmetric structure

in the middle. The orthogonal layers of metal gratings form a Fabry–Pérot-like cavity. When the polarization direction of the incident wave is perpendicular to the metal grating (x -polarized), the electromagnetic wave can be fully transmitted. When the polarization direction is parallel to the metal grating (y -polarized), the electromagnetic wave can be fully reflected. As the x -polarized wave is incident, the electromagnetic wave propagates along the oblique rectangular gap in the middle metal layer, generating polarization decomposition in the x and y directions. After the electromagnetic wave propagates to the bottom metal grating, the y -polarized wave perpendicular to the bottom metal grating will be transmitted, and the x -polarized wave will be reflected. After multiple reflections by the top and bottom metal gates, the electromagnetic wave in the F-P resonant cavity will form interference, and the beam will produce a phase effect, while the inverted beam will be cancelled. By adjusting parameters such as medium thickness, the cross polarized waves are superimposed and enhanced, while the co-polarized waves are eliminated, thereby achieving high polarization conversion rates and controlling the transmission rate of the electromagnetic waves. Compared to FSS, which requires four or even more layers to achieve a 360° phase shift range, this structure has a low profile height, which reduces the volume of the transmitarray significantly and makes it easy to integrate active devices. The traditional Tx-Rx structure is connected to the Tx-Rx part by metal fed through holes or gaps, using the principle of guided waves. The incident spatial wave is first coupled to the guided wave by the antenna. Then, the guided wave is phase shifted and finally it is reradiated, resulting in an antenna-phase shifter-antenna topology. Compared to the Tx-Rx structure, the transmission efficiency of the F-P resonant cavity is higher, and the phase response has a good linearity with frequency variation.

The current distribution, J_{surf} , when Diode 1 is turned on and Diode 2 is turned off is shown in Figure 4a. The current distribution when Diode 1 is turned off and Diode 2 is turned on is shown in Figure 4b. It can be seen that the current distribution in State 0 and State 1 is oblique symmetric at the center frequency of 5 GHz, and the current is mainly concentrated at the diode in the off state. In addition, the top and bottom metal gratings are orthogonal, and the current distribution of the entire structure is mirrored and symmetrical for State 0 and 1. The transmission amplitude responses of the two states are almost the same, and the transmission phase difference is 180° .

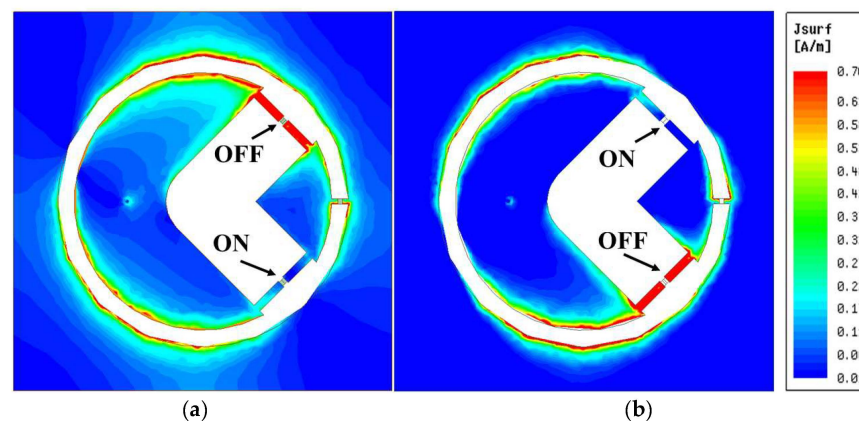


Figure 4. Unit Cell current diagram: (a) surface current distribution in State 0. (b) Surface current distribution in State 1.

2.2. Bias Line

Diodes are active devices, and their DC feeding method is generally achieved by designing additional feeding lines in the array. However, the introduction of feeding lines can affect the transmission of a unit structure, reducing transmission efficiency. Therefore, it is necessary to optimize the feeding line design. According to the equivalent circuit model, the unit needs to have two set feeding points, and the voltage difference between these two points should be ± 0.85 V, which is the working voltage of the Skyworks Solutions Inc’s SMP1340-040LF diode.

In order to achieve this function, this article adds a dielectric layer under the bottom metal gratings and designs the feeder below the dielectric layer as shown in Figure 5. In order to minimize the influence of the feeder, the direction of the feeder is designed along the x -axis, parallel to the bottom metal grating, and the feeder is extremely narrow, which gives it strong characteristics to impede microwave current. The adhesive layer is marked and highlighted with brown in Figure 5a and is between the bottom metal gratings and the feeding layer. The material used is Rogers RO4450F, exhibiting an epsilon value of 3.52. Other parameters of the unit cell include: the thickness of the feeding layer medium $h_3 = 1$ mm, the adhesive layer thickness $h = 0.1$ mm, and the total cross-sectional height of the structure is 10.6 mm, equal to 0.17λ at the central frequency. The position of the metal through-hole is $d = 5$ mm, and the inner radius of the through-hole is 0.35 mm. The structure of the bottom metal grating has been improved. In order to prevent microwave surface current from flowing to the ground through the feeder, a 10 nH inductor is installed between the circular patch in the middle layer and the outer metal ground. In theory, inductors have the highest impedance at their self-resonant frequency. When an inductor is installed on a circular groove, the circular groove will generate a higher parasitic capacitance, resulting in the total parasitic capacitance of the inductor being higher than its original parasitic capacitance. So, the self-resonant frequency of the inductor is chosen as 5.1 GHz, which is slightly higher than the center frequency. The bias circuit of the PIN diode on the substrate is shown in Figure 5. The influence of the bias circuit on S_{21} is studied through simulation, and it can be seen that the introduction of the bias circuit has a relatively small impact on the unit in the working frequency band after optimization.

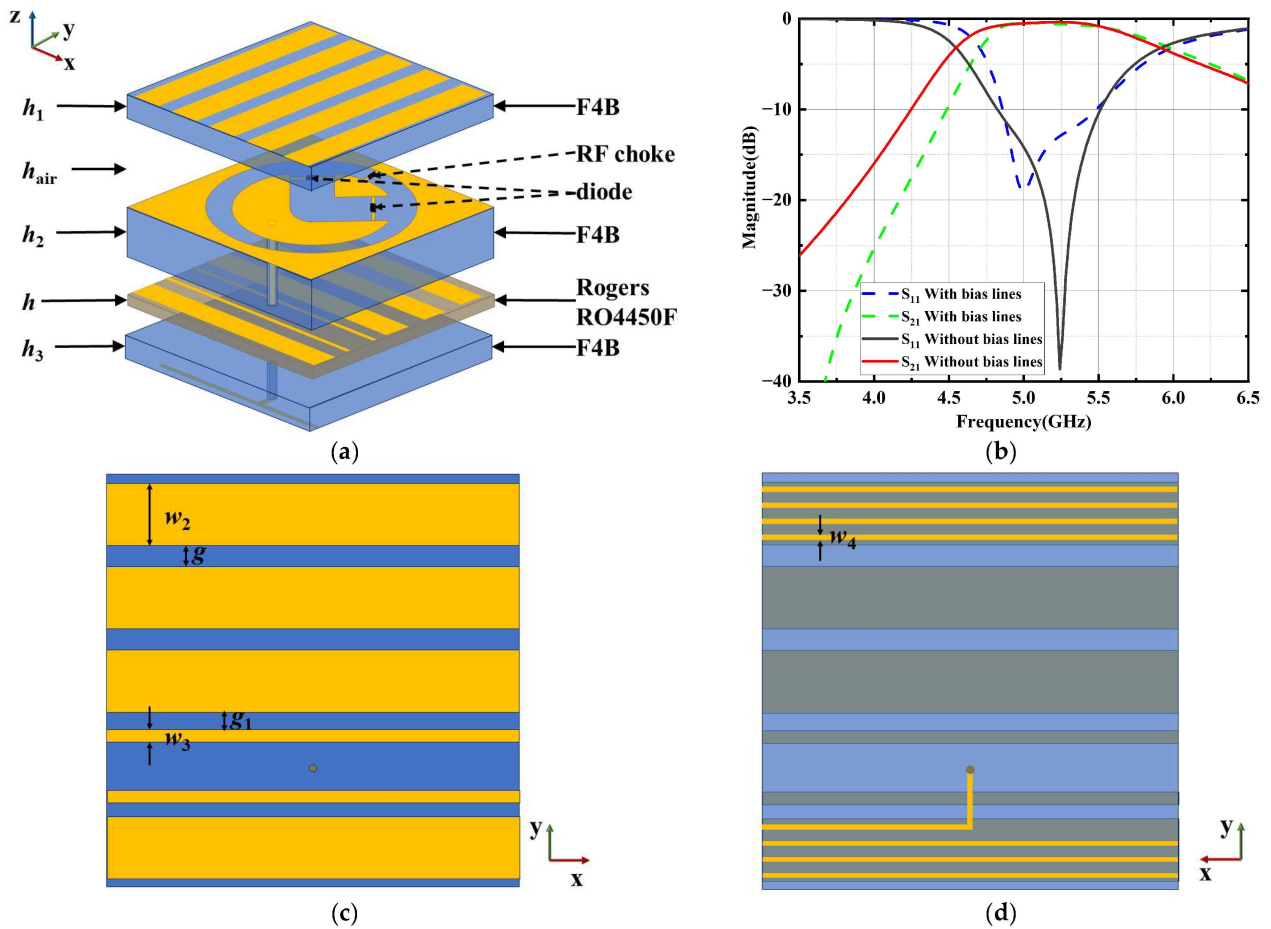


Figure 5. Comparison diagram of the transmission unit structure and simulation results before and after loading the feeding layer: (a) Side view of transmitarray unit structure with loaded feeding layer. (b) Comparison of amplitude response of transmitarray with and without feeding layer. (c) Top view of bottom metal grating. (d) Bottom view of feeding layer.

3. Transmitarray Design and Measurement

3.1. Transmitarray Beam Scanning Theory

In order to achieve two-dimensional beam scanning of the transmitarray, phase compensation needs to be applied to each unit of the transmitarray, as shown in Figure 6. The phase distribution φ_{mn} can be calculated using the following formula [25]:

$$\varphi_{mn} = -k_0 \left(\vec{R}_{mn} - \vec{u}_0 \cdot \vec{r}_{mn} \right) + \Delta\varphi \tag{1}$$

where φ_{mn} is phase distribution, $k_0 = 2\pi/\lambda_0$, λ_0 is the free space wavelength, \vec{R}_{mn} is the position vector from the phase center of the feed source to the unit, \vec{r}_{mn} is the position vector from the center of the transmitarray to the (m, n) unit, \vec{u}_0 is the direction of the transmission beam of the transmitarray, and $\Delta\varphi$ is a constant, representing the relative transmission phase. Here, we set $\Delta\varphi = 0$ for simplicity.

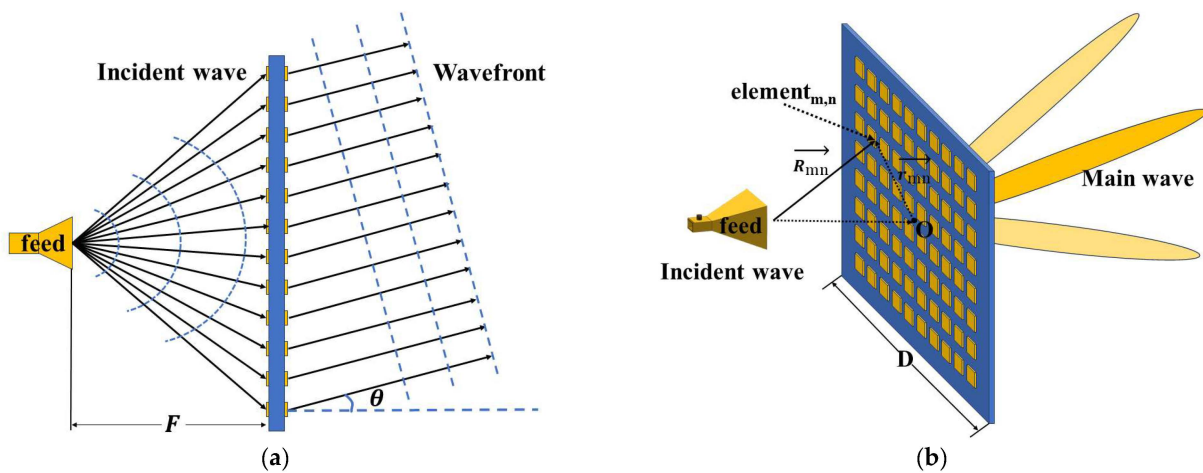


Figure 6. Schematic diagram of transmitarray antenna: (a) side view of transmitarray antenna. (b) Three-dimensional diagram of transmitarray antenna.

After calculating φ_{mn} , the 1 bit transmitarray needs to quantify φ_{mn} to the $\varphi_{q_{mn}}$. The specific quantization method is as follows:

$$\varphi_{q_{mn}} = \begin{cases} 0^\circ & -90^\circ \leq \varphi_{mn} < 90^\circ \\ 180^\circ & \text{Other} \end{cases} \tag{2}$$

According to Formula (2), $\varphi_{q_{mn}} = 0^\circ$ corresponds to State 0, and $\varphi_{q_{mn}} = 180^\circ$ corresponds to State 1 in the unit design section. The maximum quantization error caused by this method is 90° , and the average quantization error is 45° . When a two-dimensional beam scanning needs to be achieved, the compensating phase of the unit can be changed by changing the diode state, thereby achieving real-time dynamic beam scanning.

3.2. Transmitarray Design

To verify the beam scanning function of the transmitarray, the above units are used to form a 16×16 array using a horn antenna with a gain of 10 dBi as the feed source. The focal diameter ratio (F/D) is an important optimization parameter of a transmitarray. F is the distance between the phase center of the antenna feed and the center of the aperture surface of the array. D is the size of the aperture surface. Too large or too small an F/D will affect the performance of the transmitarray. When the feed antenna’s electromagnetic waves reach the aperture surface’s edge, they should be at a level of around -10 dB relative to the surface’s center to design F/D . The designed focal length F is 268 mm and the focal to diameter ratio F/D is 0.67. Each row of 16 units is divided into two groups, and sockets are designed on both sides of the antenna to connect control circuit modules. One feeding

end is provided by the through-hole linked feeder, while the other feeding end is provided by the phase control layer's cut ring patch located in the center of the unit. By designing a bias circuit, each unit can operate at ± 0.85 V and 0 V, allowing the diode to operate in two states. The operating current of each control circuit is 10 mA. The radiation pattern in both principal planes at 5 GHz can be obtained through the simulation shown in Figure 7. It can be seen that the 3 dB beam width on the E-plane is 9.7° , the sidelobe level (SLL) is -11.8 dB, and the cross-polarization level within the main lobe is below -24 dB. The 3 dB beam width on the H-plane is 9.7° , the SLL of -12.3 dB and cross-polarization level within the main lobe is below -20.7 dB.

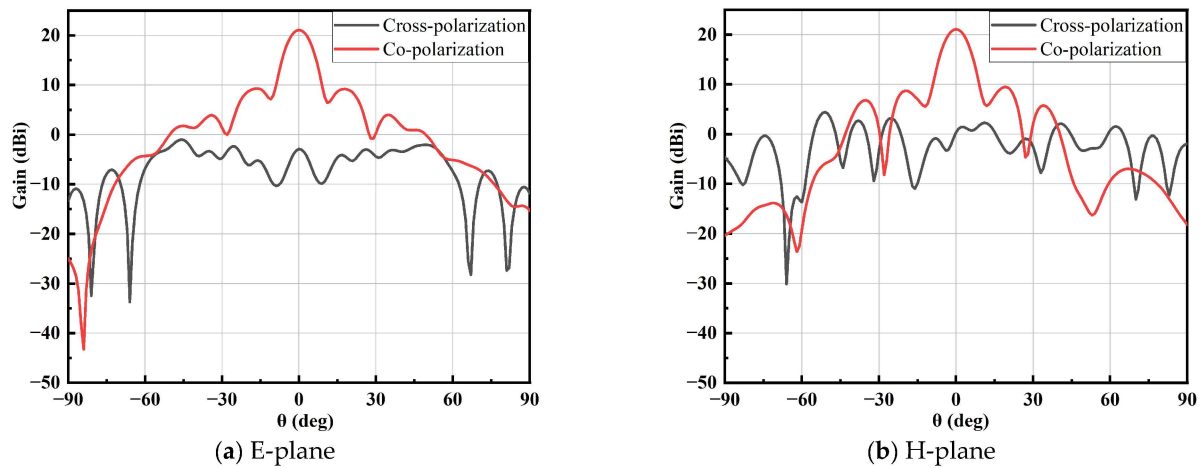


Figure 7. The radiation pattern of reconfigurable transmitarray antenna at 5 GHz. (a) E-plane simulated radiation pattern. (b) H-plane simulated radiation pattern.

3.3. Measurement Results

In order to verify the reconfigurable function of the proposed unit structure in this article, a 16×16 transmitarray, as shown in Figure 8, was manufactured and tested on the anechoic chamber. Next, the discrete phase distribution could be calculated using Formulas (1) and (2) and used to adjust the state of the diodes for beam scanning. The representative phase distribution of beam scanning angles is shown in Figure 9. As shown in Figure 10, the E-plane and H-plane's antenna patterns of $\pm 45^\circ$ beam scanning were simulated and tested.

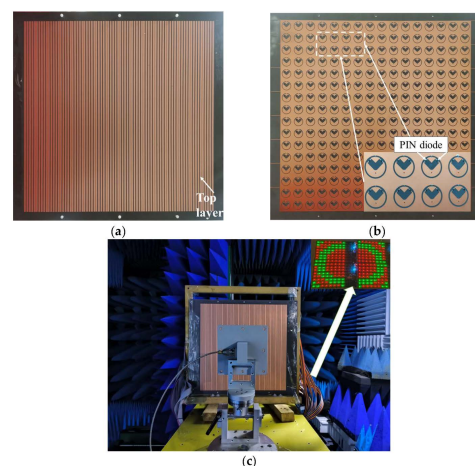


Figure 8. Fabricated prototype of transmitarray and experimental setup in the anechoic chamber. (a) Top layer. (b) Middle layer. (c) Experimental scene.

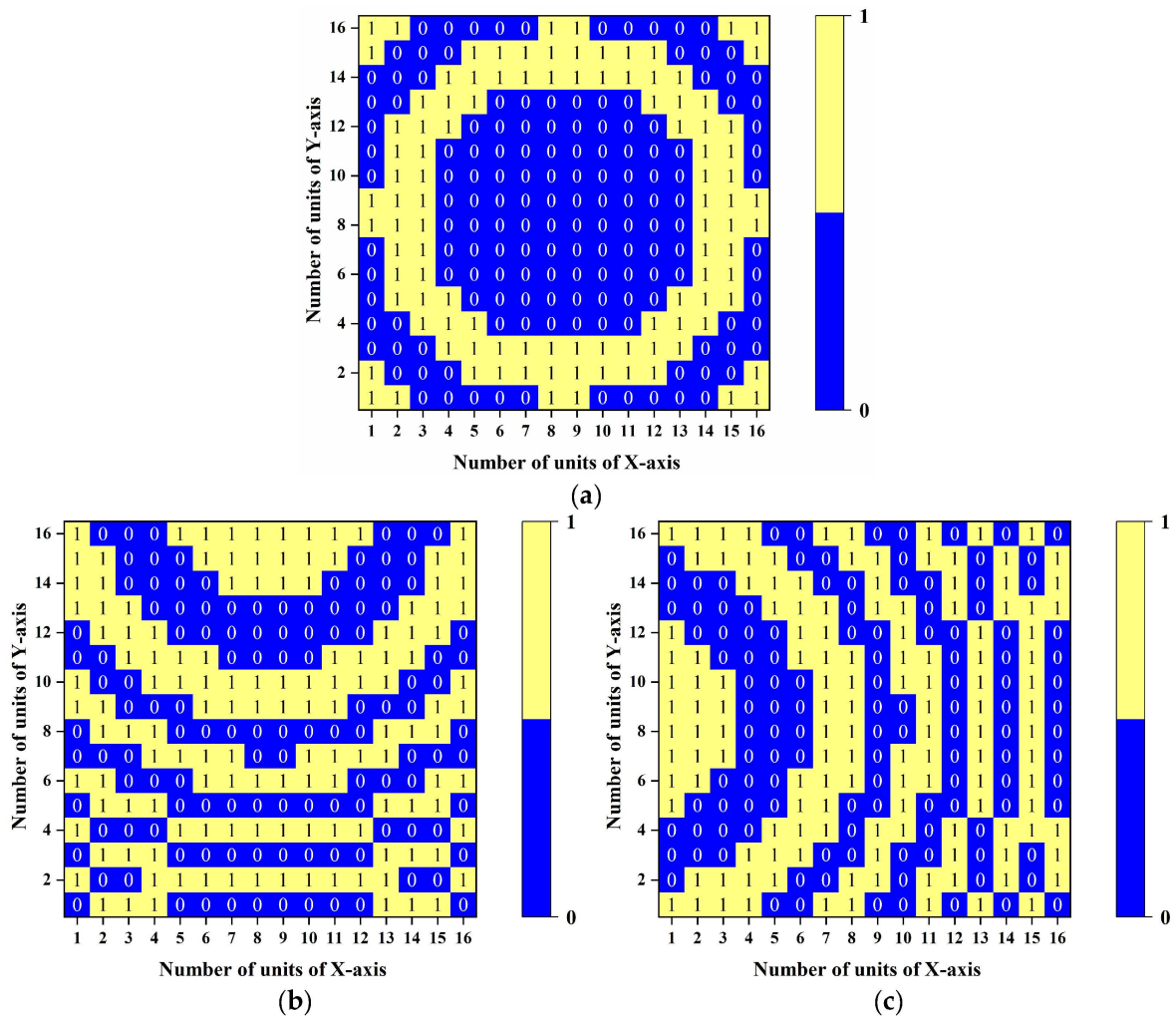


Figure 9. Phase distribution of measurement/simulated pattern for different scanning angles. (a) $\theta = 0^\circ$. (b) $\theta = 45^\circ, \varphi = 0^\circ$. (c) $\theta = 45^\circ, \varphi = 90^\circ$.

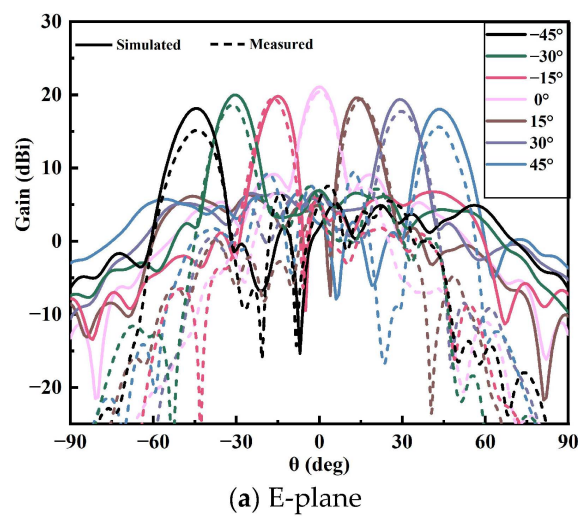


Figure 10. Cont.

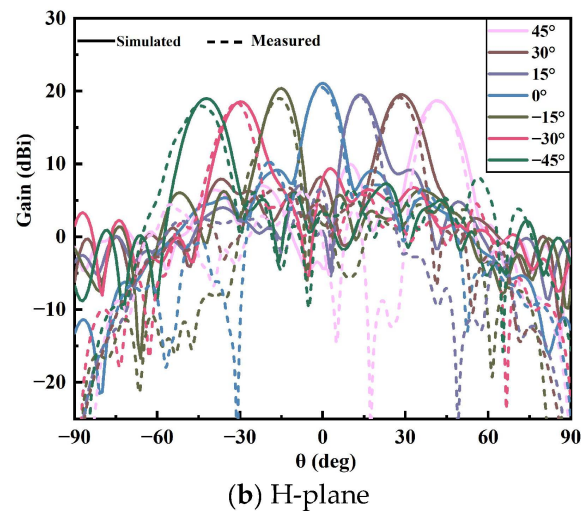


Figure 10. Reconfigurable transmitarray antenna beam scanning pattern obtained through simulation and testing at 5 GHz: (a) E-plane. (b) H-plane.

In Figure 10, it can be observed that the test results and simulation results are in good agreement. The maximum beam pointing error is within 2° due to the 1 bit quantization. When the scanning angle is large, there is a slight deviation in the beam direction. The main reason for this is that the 1 bit phase resolution accuracy is relatively lower compared to the continuous phase distribution, and there is an approximate error. The measured beam scanning angle can accurately meet the designed scanning angle. The measured beam gain gradually decreases as the scanning angle increases. In the design of transmission array, the gain and aperture efficiency are reduced due to various losses, including spillover loss, taper loss, phase quantization loss, and unit insertion loss. In addition, there are losses from fabrication and measurement errors. The measured maximum gain at 5.0 GHz is 20.59 dBi with an aperture efficiency of 20.5%, and the gain error between simulation and measurement is 0.5 dB.

The maximum losses the gain in the E-plane and H-plane are 2.96 dB and 2.11 dB at $\pm 45^\circ$ scanning angle, respectively. This is acceptable in practical applications and does not affect the overall performance of the RTA beam scanning. The above test results have verified the good beam-scanning performance of the designed reconfigurable transmitarray. A comparison of measured performance of 1 bit RTAs is given in Table 1. It can clearly be seen, that compared with the other studies from the literature shown in Table 1, the work proposed by us has a relatively high gain and aperture efficiency, and a relatively low loss when the beam scanning angle reaches 45° .

Table 1. Comparison between this work and previous research.

Ref. No.	Freq. (GHz)	Array Size (λ_0)	Max Gain (dBi)	Max Aperture Efficiency	Scanning Range and Loss	Profile Height (λ_0)
[12]	9.8	9.8×9.8	22.7	15.4%	$\pm 40^\circ$ (1.9 dB)	0.102
[3]	11.5	6.44×6.44	21.0	24.1%	$\pm 40^\circ$ (3 dB)	0.19
[18]	12.5	5.3×5.3	17.0	14.0%	$\pm 50^\circ$ (5.8 dB)	0.0875
[19]	25	0.65×0.65	17.5	20%	$\pm 40^\circ$ (3 dB)	1.7
[26]	10.5	0.28×0.28	19.8	15.9%	$\pm 60^\circ$ (5 dB)	0.125
[16]	13.5	8.6×8.6	21.4	15.4%	$\pm 60^\circ$ (3.6 dB)	0.07
This work	5.0	6.67×6.67	20.59	20.5%	$\pm 45^\circ$ (2.96 dB)	0.17

4. Conclusions

This article introduces an innovative 1 bit electronically reconfigurable transmitarray featuring a high polarization conversion rate. The core of this design lies in the strategic

use of orthogonal metal gratings to construct an F-P resonant cavity, which significantly enhances the linear polarization conversion efficiency. Central to the unit's functionality are circular gaps and patches within the middle layer, with a unit footprint of 25×25 mm ($0.42 \lambda \times 0.42 \lambda$) and a slim profile of 0.17λ . The incorporation of PIN diodes, oriented in opposite directions across the patch gaps, facilitates a 180° phase shift, ensuring that the unit exhibits a robust linear phase response across the operational bandwidth.

The practical application of this unit cell design is demonstrated through a 16×16 reconfigurable transmitarray, which successfully achieves two-dimensional beam scanning capabilities. This system is capable of adjusting the beam direction up to $\pm 45^\circ$ in both the E-plane and H-plane, with gain losses of 2.96 dB and 2.11 dB, respectively. Such performance underscores the transmitarray's exceptional gain and polarization conversion efficiency, making it an ideal candidate for advanced applications in radar and satellite communication.

Author Contributions: Conceptualization, Z.Z.; Methodology, Z.Z.; Formal analysis, Z.Z.; Investigation, W.R.; Writing—original draft, Z.Z.; Writing – review & editing, Z.Z.; Project administration, W.L.; Funding acquisition, W.R. and Z.X. All authors have read and agreed to the published version of the manuscript.

Funding: This research received no external funding.

Data Availability Statement: The raw data supporting the conclusions of this article will be made available by the authors on request.

Conflicts of Interest: The authors declare no conflict of interest.

References

1. Yusuf, Y.; Gong, X. A Low-Cost Patch Antenna Phased Array With Analog Beam Steering Using Mutual Coupling and Reactive Loading. *IEEE Antennas Wirel. Propag. Lett.* **2008**, *7*, 81–84. [[CrossRef](#)]
2. Raeesi, A.; Palizban, A.; Ehsandar, A.; Al-Saedi, H.; Gigoyan, S.; Abdel-Wahab, W.M.; Safavi-Naeini, S. A Low-Profile 2D Passive Phased-Array Antenna-in-Package for Emerging Millimeter-Wave Applications. *IEEE Trans. Antennas Propag.* **2023**, *71*, 1093–1098. [[CrossRef](#)]
3. Nguyen, B.D.; Pichot, C. Unit-Cell Loaded With PIN Diodes for 1-Bit Linearly Polarized Reconfigurable Transmitarrays. *IEEE Antennas Wirel. Propag. Lett.* **2019**, *18*, 98–102. [[CrossRef](#)]
4. Debogovic, T.; Perruisseau-Carrier, J. Low Loss MEMS-Reconfigurable 1-Bit Reflectarray Cell With Dual-Linear Polarization. *IEEE Trans. Antennas Propag.* **2014**, *62*, 5055–5060. [[CrossRef](#)]
5. Baumgartner, M.; Ghasr, M.T.; Zoughi, R. Broadband dual varactor diode-loaded elliptical slot antenna with an orthogonal feed at K-band. In Proceedings of the 2013 IEEE International Instrumentation and Measurement Technology Conference (I2MTC), Minneapolis, MN, USA, 6–9 May 2013; pp. 635–640.
6. Carrasco, E.; Barba, M.; Encinar, J.A. X-Band Reflectarray Antenna With Switching-Beam Using PIN Diodes and Gathered Elements. *IEEE Trans. Antennas Propag.* **2012**, *60*, 5700–5708. [[CrossRef](#)]
7. Ning, Y.; Zhu, S.; Chu, H.; Zou, Q.; Zhang, C.; Li, J.; Xiao, P.; Li, G. 1-Bit Low-Cost Electronically Reconfigurable Reflectarray and Phased Array Based on PIN Diodes for Dynamic Beam Scanning. *IEEE Trans. Antennas Propag.* **2023**, *72*, 2007–2012. [[CrossRef](#)]
8. Pereira, R.; Gillard, R.; Sauleau, R.; Potier, P.; Dousset, T.; Delestre, X. Dual Linearly-Polarized Unit-Cells With Nearly 2-Bit Resolution For Reflectarray Applications In X-Band. *IEEE Trans. Antennas Propag.* **2012**, *60*, 6042–6048. [[CrossRef](#)]
9. Wu, F.; Zhao, W.G.; Xia, X.; Wang, J.; Jiang, Z.H.; Sauleau, R.; Hong, W. A 2 bit Circularly Polarized Reconfigurable Reflectarray Using p-i-n-Diode-Tuned Crossed-Bowtie Patch Elements. *IEEE Trans. Antennas Propag.* **2023**, *71*, 7299–7309. [[CrossRef](#)]
10. Cuong, H.D.; Le, M.T.; Dinh, N.Q.; Tran, X.N.; Michishita, N. A Broadband 1-Bit Single-Layer Reconfigurable Reflectarray Unit Cell Based on PIN Diode Model. *IEEE Access* **2023**, *11*, 6477–6489. [[CrossRef](#)]
11. Zhou, S.G.; Zhao, G.; Xu, H.; Luo, C.W.; Sun, J.Q.; Chen, G.T.; Jiao, Y.C. A Wideband 1-Bit Reconfigurable Reflectarray Antenna at Ku-Band. *IEEE Antennas Wirel. Propag. Lett.* **2022**, *21*, 566–570. [[CrossRef](#)]
12. Clemente, A.; Dussopt, L.; Sauleau, R.; Potier, P.; Pouliguen, P. Wideband 400-Element Electronically Reconfigurable Transmitarray in X Band. *IEEE Trans. Antennas Propag.* **2013**, *61*, 5017–5027. [[CrossRef](#)]
13. Le, D.D.; Nguyen, B.D.; Nguyen, M.T.; Tran, V.S. X-band transmitarray unit-cell with 1-bit phase control. In Proceedings of the 2017 IEEE Conference on Antenna Measurements & Applications (CAMA), Tsukuba, Japan, 4–6 December 2017; pp. 385–388.
14. Nguyen, M.T.; Nguyen, B.D. 1-bit Unit-Cell For Ka-band Reconfigurable Transmitarrays. In Proceedings of the 2021 International Symposium on Antennas and Propagation (ISAP), Taipei, Taiwan, 19–22 October 2021; pp. 1–2.
15. Wang, M.; Xu, S.; Yang, F.; Hu, N.; Xie, W.; Chen, Z. A Novel 1-Bit Reconfigurable Transmitarray Antenna Using a C-Shaped Probe-Fed Patch Element With Broadened Bandwidth and Enhanced Efficiency. *IEEE Access* **2020**, *8*, 120124–120133. [[CrossRef](#)]

16. Wang, Y.; Xu, S.; Yang, F.; Li, M. A Novel 1 Bit Wide-Angle Beam Scanning Reconfigurable Transmitarray Antenna Using an Equivalent Magnetic Dipole Element. *IEEE Trans. Antennas Propag.* **2020**, *68*, 5691–5695. [[CrossRef](#)]
17. Wang, Y.; Xu, S.; Yang, F.; Werner, D.H. 1 Bit Dual-Linear Polarized Reconfigurable Transmitarray Antenna Using Asymmetric Dipole Elements With Parasitic Bypass Dipoles. *IEEE Trans. Antennas Propag.* **2021**, *69*, 1188–1192. [[CrossRef](#)]
18. Wang, M.; Xu, S.; Yang, F.; Li, M. Design and Measurement of a 1-bit Reconfigurable Transmitarray With Subwavelength H-Shaped Coupling Slot Elements. *IEEE Trans. Antennas Propag.* **2019**, *67*, 3500–3504. [[CrossRef](#)]
19. Vilenskiy, A.R.; Makurin, M.N.; Lee, C.; Ivashina, M.V. Reconfigurable Transmitarray With Near-Field Coupling to Gap Waveguide Array Antenna for Efficient 2-D Beam Steering. *IEEE Trans. Antennas Propag.* **2020**, *68*, 7854–7865. [[CrossRef](#)]
20. Grady, N.K.; Heyes, J.E.; Chowdhury, D.R.; Zeng, Y.; Reiten, M.T.; Azad, A.K.; Taylor, A.J.; Dalvit, D.A.R.; Chen, H.T. Broadband and high-efficiency terahertz metamaterial linear polarization converters. In Proceedings of the 2013 38th International Conference on Infrared, Millimeter, and Terahertz Waves (IRMMW-THz), Mainz, Germany, 1–6 September 2013; pp. 1–3.
21. Yin, L.; Xue, Z.; Ren, W.; Lv, Q.; Zhang, B.; Jin, C. High-Roll-Off-Rate Ultrathin Polarization-Rotating Frequency Selective Surface. *IEEE Antennas Wirel. Propag. Lett.* **2023**, *22*, 1592–1596. [[CrossRef](#)]
22. Yin, L.; Jin, C.; Lv, Q.; Zhang, B.; Cao, K.; Zhang, P.; Xue, Z. Amplitude and Phase Independently Adjustable Transmitarray Aperture and Its Applications to High Gain and Low Sidelobe Antenna. *IEEE Trans. Antennas Propag.* **2022**, *70*, 4498–4506. [[CrossRef](#)]
23. Yu, H.; Su, J.; Li, Z.; Yang, F. A Novel Wideband and High-Efficiency Electronically Scanning Transmitarray Using Transmission Metasurface Polarizer. *IEEE Trans. Antennas Propag.* **2022**, *70*, 3088–3093. [[CrossRef](#)]
24. Abdelrahman, A.H.; Elsherbeni, A.Z.; Yang, F. Transmission Phase Limit of Multilayer Frequency-Selective Surfaces for Transmitarray Designs. *IEEE Trans. Antennas Propag.* **2014**, *62*, 690–697. [[CrossRef](#)]
25. Abdelrahman, A.H.; Yang, F.; Elsherbeni, A.Z. *Analysis and Design of Transmitarray Antennas*; Morgan & Claypool Publishers: New York, NY, USA, 2017.
26. Diaby, F.; Clemente, A.; Sauleau, R.; Pham, K.T.; Dussopt, L. 2 Bit Reconfigurable Unit-Cell and Electronically Steerable Transmitarray at $\text{\$Ka\$}$ -Band. *IEEE Trans. Antennas Propag.* **2020**, *68*, 5003–5008. [[CrossRef](#)]

Disclaimer/Publisher’s Note: The statements, opinions and data contained in all publications are solely those of the individual author(s) and contributor(s) and not of MDPI and/or the editor(s). MDPI and/or the editor(s) disclaim responsibility for any injury to people or property resulting from any ideas, methods, instructions or products referred to in the content.